

Extreme Compression of Large Language Models via Additive Quantization

Vage Egiazarian^{*12} Andrei Panferov^{*12} Denis Kuznedelev²³ Elias Frantar⁴ Artem Babenko² Dan Alistarh⁴⁵

Abstract

The emergence of accurate open large language models (LLMs) has led to a race towards quantization techniques for such models enabling execution on end-user devices. In this paper, we revisit the problem of “extreme” LLM compression—defined as targeting extremely low bit counts, such as 2 to 3 bits per parameter, from the point of view of classic methods in Multi-Codebook Quantization (MCQ). Our work builds on top of *Additive Quantization*, a classic algorithm from the MCQ family, and adapts it to the quantization of language models. The resulting algorithm advances the state-of-the-art in LLM compression, outperforming all recently-proposed techniques in terms of accuracy at a given compression budget. For instance, when compressing LLAMA 2 models to 2 bits per parameter, our algorithm quantizes the 7B model to 6.93 perplexity (a 1.29 improvement relative to the best prior work, and 1.81 points from FP16), the 13B model to 5.70 perplexity (a .36 improvement) and the 70B model to 3.94 perplexity (a .22 improvement) on WikiText2. We release our implementation of Additive Quantization for Language Models AQLM as a baseline to facilitate future research in LLM quantization.

1. Introduction

The rapid advancement of generative large language models (LLMs) has led to massive industrial and popular interest, driven in part by the availability of accurate *open* LLMs, such as Llama 1 and 2 (Touvron et al., 2023), Falcon (TII UAE, 2023), BLOOM (Scao et al., 2022), OPT (Zhang et al., 2022), or NeoX/Pythia (Biderman et al., 2023).

A key advantage of such open models is that they can be inferred or fine-tuned locally by end-users, assuming that their computational and memory costs can be brought down

^{*}Equal contribution ¹HSE University ²Yandex Research ³Skoltech ⁴IST Austria ⁵NeuralMagic. Correspondence to: <dan.alistarh@ist.ac.at>.

Preliminary work. To be extended with additional experiments.

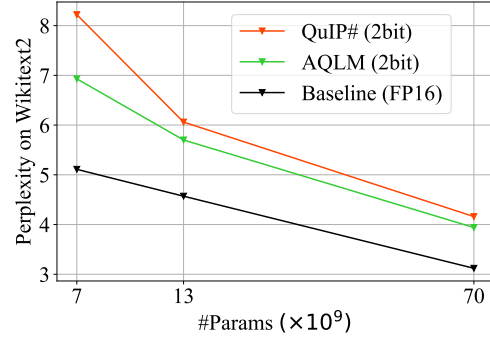


Figure 1: Comparison of AQLM (2-bit) against QuIP# (2-bit) and the original 16-bit weights on LLAMA 2 models.

to be manageable on commodity hardware. Consequently, this has led to interest in methods for inference and fine-tuning on compressed LLMs (Dettmers et al., 2022; Frantar et al., 2022a; Dettmers & Zettlemoyer, 2022; Lin et al., 2023; Dettmers et al., 2023a). Currently, the primary approach for accurate post-training compression of LLMs is *quantization*, which reduces the bit-width at which model weights (and possibly activations) are stored, leading to improvements in model footprint and memory transfer.

By and large, the general approach to LLM weight compression can be described as “direct” quantization, in the sense that a suitable quantization grid and normalization are first chosen for each matrix sub-component, and then weights are mapped onto the grid either by direct rounding, e.g. (Dettmers & Zettlemoyer, 2022), or via more complex allocations, e.g. (Frantar et al., 2022a). Quantization induces a natural compression-vs-accuracy trade-off, usually measured in terms of bits-per-element versus model perplexity (PPL). State-of-the-art approaches can achieve arguably low accuracy loss at 3-4 bits per element (Dettmers et al., 2023b; Chee et al., 2023; Kim et al., 2023), and can even stably compress models to 2 bits per element. Yet, with current methods, low bit counts come at the cost of significant drops in accuracy, higher implementation complexity and runtime overheads. Specifically, from a practitioner’s perspective, “extreme” quantization in the 2-bit range using current techniques is inferior to simply using a smaller base model and quantizing it to higher bitwidths, such as 3-4 bits per parameter, as the latter approach usually yields higher accuracy given the same model size in bytes (Dettmers &

Zettlemoyer, 2022; Chee et al., 2023).

In this work, we aim to improve the state-of-the-art in the high-compression range. We investigate an alternative approach to LLM compression, by extending *Multi-Codebook Quantization (MCQ)* to LLMs: broadly, MCQ is a family of methods developed in the context of information retrieval and approximate nearest-neighbor (ANN) search (Chen et al., 2010; Jegou et al., 2010; Ge et al., 2013; Zhang et al., 2014; Babenko & Lempitsky, 2014; Martinez et al., 2016; 2018), consisting of specialized quantization algorithms to compress databases of vectors, allowing for efficient search against this database. Unlike direct quantization algorithms, vector quantization compresses multiple values together, by leveraging the mutual information of quantized values.

Throughout this paper, we extend vector quantization from approximate nearest neighbor search to the task of compressing LLM weights with low compression error. More specifically, we adapt Additive Quantization (AQ) (Babenko & Lempitsky, 2014; Martinez et al., 2016) — a popular vector quantization algorithm — to the task of compressing LLM weights such that the output of each layer and Transformer block is approximately preserved. To that end, we reformulate the AQ optimization problem to reduce the error in LLM layer outputs, rather than preserving the weights themselves. We refer to the resulting procedure as Additive Quantization of Language Models (AQLM). Unlike other extreme LLM quantization approaches (Kim et al., 2023; Dettmers et al., 2023b), AQ quantizes models in a simple homogeneous format, which should be easy to implement in practice. The main contributions of this work can be summarized as follows:

1. We propose a practical adaptation of Additive Quantization to the task of post-training quantization of LLMs. Our technical contribution is two-fold: (1) we adapt the underlying optimization problem (specifically, a Map MRF) to be instance-aware, taking layer calibration input & output activations into account; (2) we complement the layer-wise optimization with an efficient intra-layer tuning technique, which optimizes quantization parameters jointly over several layers, using only the calibration data.
2. We evaluate the effectiveness of this algorithm on the task of compressing 7-70B parameter LLMs from the Llama2 family (Touvron et al., 2023) with compression rates of 2-4 bits per parameter. We find that AQLM outperforms the previous state-of-the-art algorithm across the 2-4 bit compression, with most significant improvements for extreme 2-bit quantization.
3. To facilitate reproducibility, we publish the reference implementation¹ of AQLM, along with several pre-quantized models.

¹<https://github.com/vahe1994/AQLM>

2. Background & Related Work

2.1. LLM Quantization

We first overview work on post-training quantization (PTQ) methods (Nagel et al., 2020; Gholami et al., 2021) in the context of LLMs. Broadly, while there is significant work on classic PTQ techniques such as AdaRound (Nagel et al., 2020), BitSplit (Wang et al., 2020), AdaQuant (Hubara et al., 2021), BRECQ (Li et al., 2021), and OBQ (Frantar et al., 2022b); these methods primarily focus on accurate quantization of smaller models, e.g. in the 10-100M range, and are hard to scale for LLMs due to the computational demands of their underlying solvers for billion-scale models.

Early efforts towards PTQ methods that scale to LLMs such as ZeroQuant (Yao et al., 2022), LLM.int8() (Dettmers et al., 2022), and nuQmm (Park et al., 2022) employed direct round-to-nearest (RTN) projections, and adjusted quantization granularity to balance memory efficiency and accuracy. GPTQ (Frantar et al., 2022a) proposed a more accurate *data-aware approach* by leveraging an approximate large-scale solver for minimizing layer-wise ℓ_2 errors.

Dettmers et al. (Dettmers & Zettlemoyer, 2022) examined the accuracy-compression trade-offs of these early methods, suggesting that 4-bit quantization may be optimal for RTN quantization, and observing that data-aware methods like GPTQ allow for higher compression, i.e. strictly below 4 bits per weight, still maintaining Pareto optimality. Parallel work quantizing both weights *and activations* to 8-bits, by Dettmers et al. (2022), Xiao et al. (2022), and Yao et al. (2022) yielded insights into the sources of quantization error, notably the fact that the “outlier features” in large LLMs cause substantial quantization errors, prompting various mitigation strategies.

Following this initial wave of work on LLM quantization, several improved techniques have been proposed, mainly focusing on the difficulty of quantizing outliers in the weight matrix. SpQR (Dettmers et al., 2023b) addresses this by saving the outlier weights—which have disproportionately high impact on the output error—as a highly-sparse higher-precision matrix. AWQ (Lin et al., 2023) reduces the error of quantizing channels with the highest activation magnitudes by employing per-channel scaling to reduce the error on important weights. SqueezeLLM (Kim et al., 2023) uses the diagonal Fisher as a proxy for the Hessian and implements non-uniform quantization through K-means clustering. This method identifies outliers as large entries, or entries sensitive to quantization, retaining them in original precision.

Currently, the state-of-the-art method in terms of accuracy-to-size trade-off is QuIP (Chee et al., 2023), and its newer variant QuIP# (Tseng et al.). Roughly, these methods work by first “smoothing” outliers by multiplying with a rotation matrix (e.g., a Hadamard transform), and then mapping

the smoothened weights onto a lattice via a projection procedure. QuIP was the first method to obtain stable results (i.e., single-digit PPL increases) in the 2-bit per parameter compression range.

At a high level, these methods aim to minimize the “worst-case” quantization error for each layer, given initial weights and calibration data. For instance, in QuIP#, the distribution of the rotated weights approximates a Gaussian distribution, while the encoding lattice (E8P) is chosen to minimize the “rounding” error. By contrast, our approach uses a different weight encoding (codebooks are used additively), and *learned* codebooks instead of a fixed codebook, leveraging the intuition that we should be able to obtain better encoding by direct optimization. In the same vein, we allow codebooks for different layers to co-train via a separate fine-tuning procedure.

2.2. Quantization for Nearest Neighbor Search

Our investigation builds on a different family of quantization algorithms designed for approximate nearest neighbor search (ANN). Unlike PTQ, the main objective of ANN quantization is to compress a database of vectors in a way that allows user to efficiently compute similarities and find nearest neighbors, typically in terms of euclidean distance or inner product, relative to a set of query points. To achieve high compression rates, modern ANN search algorithms can use *vector quantization* (VQ) — a technique that quantizes multiple vector dimensions together, as a vector (Burton et al., 1983; Gray, 1984). It achieves this by learning “codebooks”: a codebook is a set of learnable candidate vectors that can be used to encode the data.

To encode a given database vector, VQ splits it into subgroups of several dimensions each, then encodes every group by choosing a vector from the learned codebook. The algorithm was designed to efficiently compute distances or dot-products for similarity search by taking advantage of the linear properties of dot products.

Modern quantization methods for ANN search generalize the idea of vector quantization and are referred to as multi-codebook quantization (MCQ) in the literature. MCQ methods typically do not involve the information loss on the query side, what makes them the leading paradigm for the memory-efficient ANN (Ozan et al., 2016; Martinez et al., 2018). We review several MCQ variants below.

Product quantization (PQ) (Jegou et al., 2010) is a pioneering method from the MCQ family, which encodes each vector $x \in \mathbf{R}^D$ as a concatenation of M codewords from M $\frac{D}{M}$ -dimensional codebooks C_1, \dots, C_M , each containing K codewords. Simply put, PQ decomposes a vector into M separate subvectors and applies vector quantization (VQ) to each subvector, while using a separate codebook. As a result,

each vector x is encoded by a tuple of codeword indices $[i_1, \dots, i_M]$ and approximated by $x \approx [c_{1i_1}, \dots, c_{Mi_M}]$. Fast Euclidean distance computation becomes possible using lookup tables:

$$\|q - x\|^2 \approx \|q - [c_{1i_1}, \dots, c_{Mi_M}]\|^2 = \sum_{m=1}^M \|q_m - c_{mi_m}\|^2 \quad (1)$$

where q_m is the m th subvector of a query q . This sum can be calculated using M additions and lookups if the distances from query subvectors to codewords are precomputed.

Geometrically, PQ effectively partitions the original vector space into K^M “cells,” each being a Cartesian product of M lower-dimensional cells. Such product-based approximation works better if the $\frac{D}{M}$ -dimensional components of vectors have independent distributions. The degree of dependence is affected by the choice of the splitting, and can be further improved by orthogonal transformation applied to vectors as pre-processing. Two subsequent works have therefore looked into finding an optimal transformation (Ge et al., 2013; Norouzi & Fleet, 2013). Modifications of PQ corresponding to such pre-processing transformations are referred below as Optimized Product Quantization (OPQ).

Non-orthogonal quantizations. Follow-up works (Chen et al., 2010; Babenko & Lempitsky, 2014; Martinez et al., 2016; Zhang et al., 2014; Ozan et al., 2016; Martinez et al., 2018) generalized the idea of Product Quantization by approximating each vector by a *sum* of M codewords instead of concatenation. The resulting procedure is still efficient while the approximation accuracy is increased.

The first approach, Residual Vector Quantization (Chen et al., 2010), quantizes original vectors, and then iteratively quantizes the approximation residuals from the previous iteration. Another approach, Additive Quantization (AQ) (Babenko & Lempitsky, 2014), is the most general as it does not impose any constraints on the codewords from the different codebooks. Usually, AQ provides the smallest compression errors, however, it is much slower than other methods, especially for large M . This is because AQ relies on an iterative two-phase optimization procedure that alternates between updating codebooks and re-encoding the database. Since this procedure is central to our work, we discuss it in more detail in Section 3.

Finally, several recent works (Martinez et al., 2016; 2018; Zhang et al., 2014) elaborate the idea of Additive Quantization, proposing the more effective procedure for codebooks learning. Composite Quantization (CQ) (Zhang et al., 2014) learns codebooks with a fixed value of scalar product between the codewords from different codebooks. Currently, state-of-the-art compression accuracy is achieved by the LSQ method (Martinez et al., 2018).

Vector quantization for model compression. There has been significant work on exploiting vector quantization in the context of machine learning. For instance, Zhou et al. (2017); Li et al. (2017); Chen et al. (2019) use multi-codebook quantization to compress word embeddings within deep learning models. Another line of work (Blalock & Gutttag, 2021; McCarter & Dronen, 2022; Fernández-Marqués et al., 2023) explores vector quantization for linear models, or linear layers within deep models. Similarly to PQ above, these techniques pre-compute inner products between inputs and all codes, then compute linear layer via look-up, which speeds up inference. However, these algorithms introduce significant prediction error that does not allow them to compress deep models. In this context, we are the first to successfully adapt MCQ approaches to LLMs.

3. AQLM: Additive Quantization for LLMs

3.1. Overview

Our algorithm starts from the intuition that additive quantization (AQ) aims to solve a similar problem to standard approaches in post-training quantization (PTQ) (Nagel et al., 2020; Frantar et al., 2022b): specifically, both settings assume the existence of a set of “input” vectors, i.e. input data for AQ, and the weight matrix rows for PTQ. The goal is to compress these inputs while preserving dot product similarity, against query vectors (for AQ), and against layer input embeddings (for PTQ). The difference between the two is that, AQ normally assumes that the distribution of queries is unknown, whereas PTQ methods such as OBC (Frantar et al., 2022b) optimize for specific input embeddings chosen from a set of calibration data.

In the rest of this section, we present an adaptation of AQ in the context of neural network compression, by taking into account the distribution over input activations. Specifically, for a linear layer with d_{in} input and d_{out} output features given its weights $\mathbf{W} \in \mathbb{R}^{d_{out} \times d_{in}}$ and a set of calibration inputs $\mathbf{X} \in \mathbb{R}^{d_{in} \times n}$, one seeks for a configuration of quantized weights $\hat{\mathbf{W}}$ that optimizes squared error between the output of the original and compressed layer:

$$\arg \min_{\hat{\mathbf{W}}} \|\mathbf{W}\mathbf{X} - \hat{\mathbf{W}}\mathbf{X}\|_2^2. \quad (2)$$

In the following, we will assume that $\hat{\mathbf{W}}$ is quantized using AQ, and adopt standard notation (Martinez et al., 2016). The AQ scheme splits weight rows into groups of g consecutive elements, and represents each group of weights as a sum of M vectors chosen from multiple learned codebooks C_1, \dots, C_M , each codebook containing 2^B vectors (for B-bit codes). A weight is encoded by choosing a single code from each codebook and summing them up. For simplicity, we denote this choice as a one-hot vector b_m , which results in the following representation for a group: $\sum_{m=1}^M C_m b_{i,j,m}$.

This is similar to PTQ algorithms such as GPTQ (Frantar et al., 2022a), except for having more complex coding for each group. In contrast, GPTQ can be seen as quantizing each group to a separate code.

To represent the full weight, we simply concatenate:

$$\hat{\mathbf{W}}_i = \sum_{m=1}^M C_m b_{i,1,m} \oplus \dots \oplus \sum_{m=1}^M C_m b_{i,d_{in}/g,m} \quad (3)$$

Here, \oplus denotes concatenation and $b_{ijm} \in \mathbb{R}^{2^B}$ represents a one-hot code for the i -th output unit, j -th group of input dimensions and m -th codebook.

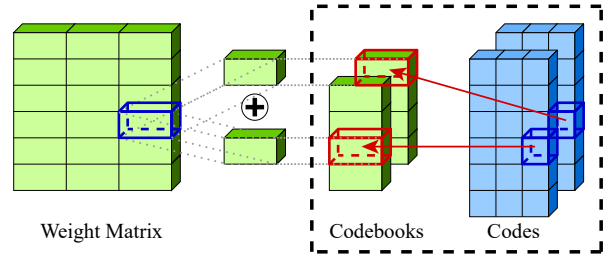


Figure 2: Groups of weights are represented by a sum of codes selected from codebooks by corresponding indices.

Our algorithm will learn codebooks $C_m \in \mathbb{R}^{g \times 2^B}$ and the discrete codes represented by one-hot $b \in \mathbb{R}^{d_{out} \times d_{in}/g \times M \times 2^B}$. The resulting scheme encodes each group of g weights using $M \cdot B$ bits and further requires $g \cdot 2^B \cdot 16$ bits for FP16 codebooks. The compression error to be minimized becomes:

$$\arg \min_{C,b} \|\mathbf{W}\mathbf{X} - \left(\text{Concat}_{i,j} \sum_{m=1}^M C_m b_{i,j,m} \right) \mathbf{X}\|_2^2. \quad (4)$$

To learn this weight representation, we initialize codebooks C and codes b by running residual K-means following (Chen et al., 2010). Then, we alternate between updating codes $b_{i,j,m}$ and codebooks C_m until the loss function (4) stops improving up to the specified tolerance. Since codes are discrete and codebooks are continuous, optimizing them requires two distinct optimization strategies. We describe each of these two optimization phases below.

3.2. Phase 1: Beam search for codes

During this phase, AQ updates the codes $b_{i,j,m}$ to minimize the MSE objective (4). Similarly to Babenko & Lempitsky (2014); Martinez et al. (2016; 2018), we reformulate the objective in terms of a fully-connected discrete Markov Random Field (MRF) to take advantage of MRF solvers.

To simplify the derivation, let us first consider a special case where there is a single output unit ($d_{out}=1$) and a single quantization group (i.e. $g=d_{in}$), to get rid of the

concatenation operator: $\|\mathbf{W}\mathbf{X} - \sum_{m=1}^M C_m b_m \mathbf{X}\|_2^2$. We rewrite this objective by expanding the squared difference²:

$$\begin{aligned} \|\mathbf{W}\mathbf{X} - \sum_{m=1}^M C_m b_m \mathbf{X}\|_2^2 &= \|\mathbf{W}\mathbf{X}\|_2^2 - \\ &- 2 \left\langle \mathbf{W}\mathbf{X}, \sum_{m=1}^M C_m b_m \mathbf{X} \right\rangle_F + \left\| \sum_{m=1}^M C_m b_m \mathbf{X} \right\|_2^2 \end{aligned} \quad (5)$$

Here, the $\langle \cdot, \cdot \rangle_F$ denotes a Frobenius inner product of two matrices. Intuitively, this is defined as an inner product between the vectors obtained by flattening the two matrices, or equivalently, $\langle \mathbf{A}, \mathbf{B} \rangle_F = \langle \text{vec}(\mathbf{A}), \text{vec}(\mathbf{B}) \rangle = \text{tr}(\mathbf{A}^T \mathbf{B})$.

Let us consider the three components of (5) in isolation. First, note that $\|\mathbf{W}\mathbf{X}\|_2^2$ is constant in b and can be disregarded during optimization. The second component can be expanded further into pairwise dot products:

$$\left\| \sum_{m=1}^M C_m b_m \mathbf{X} \right\|_2^2 = \sum_{i=1}^M \sum_{j=1}^M \langle C_i b_i \mathbf{X}, C_j b_j \mathbf{X} \rangle_F. \quad (6)$$

Note that both the second and third components rely on Frobenius products of $C_m b_m \mathbf{X}$ -like matrices. These matrices can be inconvenient in practice: since $\mathbf{X} \in \mathbb{R}^{d_{in} \times n}$, the size of each matrix will scale with the size of calibration dataset n . To circumvent this, we rewrite the products as:

$$\langle C_i b_i \mathbf{X}, C_j b_j \mathbf{X} \rangle_F = \langle C_i b_i \mathbf{X} \mathbf{X}^T, C_j b_j \rangle_F. \quad (7)$$

In this form, it is clear that one can pre-compute $\mathbf{X} \mathbf{X}^T \in \mathbb{R}^{d_{in} \times d_{in}}$. Abusing notation, we denote this type of product as $\langle \mathbf{A}, \mathbf{B} \rangle_{\mathbf{X} \mathbf{X}^T} \stackrel{\text{def}}{=} \langle \mathbf{A} \mathbf{X} \mathbf{X}^T, \mathbf{B} \rangle_F$ in future derivations.

Combining all these derivations, equation (5) becomes:

$$\begin{aligned} \|\mathbf{W}\mathbf{X} - \sum_{m=1}^M C_m b_m \mathbf{X}\|_2^2 &= \|\mathbf{W}\mathbf{X}\|_2^2 - \\ &- 2 \sum_{m=1}^M \langle \mathbf{W}, C_m b_m \rangle_{\mathbf{X} \mathbf{X}^T} + \sum_{i=1}^M \sum_{j=1}^M \langle C_i b_i, C_j b_j \rangle_{\mathbf{X} \mathbf{X}^T}. \end{aligned} \quad (8)$$

Finally, we generalize this equation to multiple output units ($d_{out} > 1$) and quantization groups ($g \neq d_{in}$). For $d_{out} > 1$, note that the original objective (4) is additive with respect to output units: thus, we can apply (8) independently to each output dimension and add up results. To support multiple input groups ($g \neq d_{in}$), we can treat each group as a separate codebook where only the codes for the active group are nonzero. Thus, we need to repeat each codebook d_{in}/g times and pad it with zeros according to the active group.

²Best viewed as a tensor generalization of the following equation: $(a - b)^2 = a^2 + b^2 - 2ab$

It is now evident that minimizing (5) is equivalent to MAP inference in a Markov Random Field with $\langle \mathbf{W}, C_m b_m \rangle_{\mathbf{X} \mathbf{X}^T}$ as unary potentials and $\langle C_i b_i, C_j b_j \rangle_{\mathbf{X} \mathbf{X}^T}$ as pairwise potentials. While finding the exact optimum is infeasible, prior work has shown that this type of MRF can be solved approximately with beam search or ICM (Besag, 1986).

To solve this problem, we chose to adapt a beam search algorithm from Babenko & Lempitsky (2014). This algorithm maintains a beam of k (beam size) best configurations for the codes, starting from the previous solution. On each step, the algorithm attempts to replace one code by trying all $2^B k$ alternatives and selecting the k best based on MSE (8).

Since the loss function is additive, changing one code only affects a small subset of loss components. Thus, we can compute the loss function efficiently by starting with a previous loss function (before code replacement), then adding and subtracting the components that changed during this iteration. These few loss components can be computed efficiently by multiplying with $\mathbf{X} \mathbf{X}^T$ ahead of beam search. The beam search runs over all d_{out} output units in parallel. This is possible because encoding one output unit does not affect the objective (8) of other units. Note that beam search is not the best known solution to this problem. Modern AQ variants for retrieval (Martinez et al., 2016; 2018) use randomized ICM to find solutions faster. In this study, we chose beam search only because it was easier to implement in high-level frameworks like PyTorch/JAX.

3.3. Phase 2: Codebook update

In the second phase, we find the optimal codebook vectors C_1, \dots, C_M that minimize the same squared error as beam search. Note that, if we treat the codes b as constants, minimizing (4) becomes a least squares problem for C_m . The original AQ algorithm solves this problem in a closed form, relying on the fact that each vector dimension can be optimized independently.

Our problem is more complicated because of the presence of $\mathbf{X} \mathbf{X}^T$: the optimal value of one codebook coordinate depends on the values of all other coordinates. In principle, we could still optimize C_m in a closed form, but it would require inverting an impractically large matrix. We can also use iterative least squares solvers (e.g. conjugate gradients) specialized for this type of problem.

For simplicity, our current implementation defaults to using Adam (Kingma & Ba, 2015) for approximately solving this minimization problem. In practice, this codebook tuning phase takes up a small fraction of the total compute time. We compute the objective as follows:

$$\begin{aligned} \|\mathbf{W}\mathbf{X} - \widehat{\mathbf{W}}\mathbf{X}\|_2^2 &= \|(\mathbf{W} - \widehat{\mathbf{W}})\mathbf{X}\|_2^2 = \\ &= \left\langle (\mathbf{W} - \widehat{\mathbf{W}})\mathbf{X} \mathbf{X}^T, (\mathbf{W} - \widehat{\mathbf{W}}) \right\rangle_F, \end{aligned} \quad (9)$$

where $\widehat{\mathbf{W}}$ is the quantized weight matrix from 3, and the \mathbf{XX}^T matrix is pre-computed. We optimize this objective by iterating (non-stochastic) full-batch gradient descent.

For each codebook update phase, our implementation runs 100 Adam steps with learning rate $1e-4$. However, we found that the final result is not sensitive to either of these parameters: training with smaller number of steps or learning rate achieves the same loss, but takes longer to converge. In future work, these hyperparameters could be eliminated by switching to dedicated least squares solver for codebooks.

Similarly to most other quantization algorithms, we also learn per-unit scales $s \in \mathbb{R}^h$ that are initialized as $s_i := \|\mathbf{W}_i\|_2$ and updated alongside codebooks with the same Adam optimizer (line 19 in Algorithm 1).

3.4. Fine-tuning for intra-layer cohesion

So far, our algorithm compresses each weight matrix independently of the rest of the model. However, in practice, quantization errors interact differently between matrices. This issue is especially relevant in the case of for extreme (2-bit) compression, where quantization errors are larger.

Prior work addresses this issue via quantization-aware training (QAT), e.g. (Gholami et al., 2021). Instead of compressing the entire model in a single pass, they quantize model parameters gradually and train the remaining parameters to compensate for the quantization error. Unfortunately, running QAT in our setting is infeasible, since most modern LLMs are extremely expensive to train or even fine-tune. Thus, most PTQ algorithms for LLMs only adjust model parameters within the same linear layer (Frantar et al., 2022a; Lin et al., 2023; Dettmers et al., 2023b).

Here, we opt for a middle ground between the two approaches by performing optimization at the level of individual transformer blocks, i.e. groups of 4-8 linear layers³ that constitute a single multi-head self-attention, followed by a single and MLP layer. Having quantized all linear layers within a single transformer block, we fine-tune its remaining parameters to better approximate the original outputs of that transformer block by backpropagating through the weight representation (3).

More specifically, we use PyTorch autograd engine to differentiate the $\|\text{block}(\mathbf{X}_{block}) - \mathbf{Y}_{block}\|_2^2$, where \mathbf{X}_{block} are the inputs activations for that transformer block and \mathbf{Y}_{block} are output activations of $\text{block}(\mathbf{X}_{block})$ recorded prior to quantization. We train the codebooks C_m , scale vectors s and all non-quantized parameters (RMSNorm scales and biases), while keeping the codes $b_{i,j,m}$ frozen.

³The exact number depends on several of factors including the use of gated GLU activations, group query attention and QKA weight merging.

Algorithm 1 Additive Quantization for LLM

Require: model, data

```

1:  $\mathbf{X}_{block} := \text{model.input\_embeddings}(\text{data})$ 
2: for  $i = 1, \dots, \text{model.num\_layers}$  do
3:    $\text{block} := \text{model.get\_block}(i)$ 
4:    $\mathbf{Y}_{block} := \text{block}(\mathbf{X}_{block})$ 
5:   for  $\text{layer} \in \text{linear\_layers}(\text{block})$  do
6:      $\mathbf{W} := \text{layer.weight}$ 
7:      $\mathbf{X} := \text{layer\_inputs}(\text{layer}, \mathbf{X}_{block})$ 
8:      $C, b, s := \text{initialize}(\mathbf{W})$  // k-means
9:     while loss improves by at least  $\tau$  do
10:       $C, s := \text{train\_Cs\_adam}(\mathbf{XX}^T, \mathbf{W}, C, b, s)$ 
11:       $b := \text{beam\_search}(\mathbf{XX}^T, \mathbf{W}, C, b, s)$ 
12:    end while
13:    /* save for fine-tuning */
14:     $\text{layer.weight} := \text{AQFormat}(C, b, s)$ 
15:  end for
16:   $\theta := \text{trainable\_parameters}(\text{block})$ 
17:  while loss improves by at least  $\tau$  do
18:     $L := \|\text{block}(\mathbf{X}_{block}) - \mathbf{Y}_{block}\|_2^2$ 
19:     $\theta := \text{adam}(\theta, \frac{\partial L}{\partial \theta})$ 
20:  end while
21:   $\mathbf{Y}_{block} := \text{block}(\mathbf{X}_{block})$ 
22: end for
```

Similarly to Section 3.3, we train these parameters using Adam optimizer to minimize the mean squared error against the original block outputs (prior to quantization). This phase uses the same calibration data as for the individual layer quantization. The full procedure is summarized in Alg. 1.

While fine-tuning transformer blocks is more expensive than individual linear layers, it is still possible to quantize billion-parameter models on a single GPU. Furthermore, since the proposed algorithm only modifies the few remaining trainable parameters, it uses relatively little VRAM for Adam optimizer states. The fine-tuning procedure typically converges after a few epochs, likely because it starts from a good initial guess. In practice, fine-tuning transformer layers takes up a minority (10-30%) of the total calibration time. However, the entire procedure takes longer than single-pass quantization algorithms such as GPTQ.

4. Experiments

We evaluate the AQLM algorithm in typical scenarios for post-training quantization of modern LLMs. Our evaluation is focused on the LLAMA 2 model family since it is a popular backbone for fine-tuned models or general LLM applications, e.g. (Dettmers et al., 2023a). We organize the experiments as follows: in Section 4.1 we evaluate the full AQ procedure for various LLAMA 2 models and quantization bit widths, and Section 4.2 presents an ablation analysis for individual AQ components and implementation details.

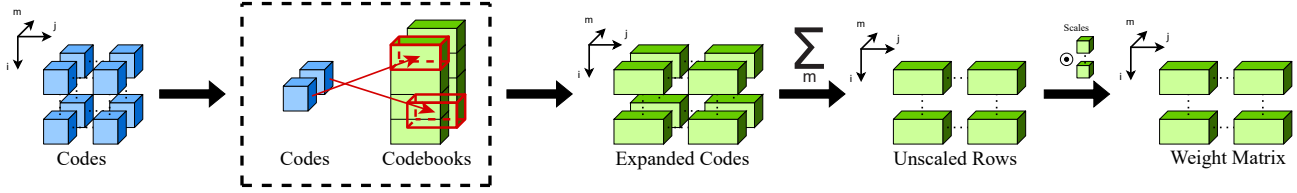


Figure 3: AQLM compressed weight format. Horizontal and vertical axes are input features and output units, respectively. Depth represents the codebook index. Reconstruction procedure, from left to right: i) compressed weight codes ii) zoom-in one weight group, each code is an index in its respective codebook iii) select codes from each codebook iv) add up codes as in (3) v) multiply by scales (one scale per output dimension).

Table 1: Evaluation of quantized Llama 2 models for **2-2.1 bits per parameter**. The table reports perplexity on WikiText2 (Merity et al., 2016) and C4 (Raffel et al., 2020), as well as accuracy for zero-shot tasks. The **Average accuracy** column is the mean of 5 zero-shot task accuracies. Primary metrics are Wiki2 (PPL), C4 (PPL) and Average accuracy.

Size	Method	Avg bits	Wiki2↓	C4↓	WinoGrande↑	PiQA↑	HellaSwag↑	ArcE↑	ArcC↑	Average accuracy↑
7B	–	16.00	5.12	6.63	67.25	78.45	56.69	69.32	40.02	62.35
	AQLM	2.02	6.93	8.84	64.64	73.50	48.23	62.84	33.62	56.57
	QuIP	2.020	222.54	145.03	51.78	54.62	27.25	26.01	19.37	35.81
	QuIP#	2.02	8.22	11.01	62.43	71.38	42.94	55.56	28.84	52.23
13B	–	16.00	4.57	6.05	69.61	78.73	59.72	73.27	45.56	65.38
	AQLM	1.970	5.70	7.59	69.46	75.08	53.44	66.96	38.48	60.68
	QuIP	2.00	13.48	16.16	52.80	62.02	35.80	45.24	23.46	43.86
	QuIP#	2.011	6.06	8.07	63.38	74.76	51.58	64.06	33.96	57.55
70B	–	16.00	3.12	4.97	76.95	81.07	63.99	77.74	51.11	70.17
	AQLM	2.070	3.94	5.72	75.93	80.43	61.79	77.68	0.4793	68.75
	QuIP	2.01	5.90	8.17	67.48	74.76	50.45	62.16	33.96	57.76
	QuIP#	2.01	4.16	6.01	74.11	79.76	60.01	76.85	47.61	67.67

4.1. LLAMA 2 compression

To evaluate the quality of AQ-quantized models, we report perplexity on WikiText2 (Merity et al., 2016) and C4 (Raffel et al., 2020) validation sets. We also measure zero-shot accuracy on five tasks: WinoGrande (Sakaguchi et al., 2021), PiQA (Tata & Patel, 2003), HellaSwag (Zellers et al., 2019), ARC-easy and ARC-challenge (Clark et al., 2018) via the LM Evaluation Harness (Gao et al., 2021). We run all evaluations with the same hyperparameters as in GPTQ (Frantar et al., 2022a), except for the increased number of training calibration sequences.

We consider three main targets in terms of compression range: 2-2.1 bits, 3-3.1 bits, and 4-4.1 bits per model parameter. The full number of bits for each algorithm includes scales, codebooks, zero points, but not the (non-quantized) word embeddings and logits. We compare AQ against GPTQ for 3&4 bits (Frantar et al., 2022a), SpQR for 3&4 bits (Dettmers et al., 2023b), QuIP in 2,3 & 4 bits (Chee et al., 2023) and QUIP# for 2&4 bits (Tseng et al.). While GPTQ and SpQR technically support 2-bit quantization,

these algorithms were designed for 3+ bits per parameter and perform poorly in terms of accuracy in the 2-2.1 bit range. For QuIP, we omit results for the 7B model, as we could not achieve competitive performance in this one scenario using the available⁴ implementations. For QuIP#, we focus on 2 and 4 bit because the available implementation does not yet support 3-bit compression. While there are several ways to modify QuIP to support 3 bits, it is unclear which way is more natural. We calibrate each quantization algorithm using the same portion of RedPajama calibration dataset (Computer, 2023), with a sequence length of 4096.

We report the results in Tables 1 2 and 3 (for 2, 3 and 4 bits respectively), both in terms of perplexity and zero-shot accuracy. To summarize, AQLM outperforms the previous best PTQ algorithms across all settings, but the margin of improvement varies significantly. For example, we observe the highest gains in perplexity in the “extreme” 2-2.1 bits per

⁴Unfortunately, there is no official implementation of the original QuIP (non-#) for the LLAMA 2 model, see <https://github.com/Cornell-RelaxML/QuIP/issues/2>.

Extreme LLM Compression of Using Additive Quantization

Table 2: Evaluation of quantized Llama 2 models for **3-3.1 bits per parameter**. The table reports perplexity on Wiki-Text2 (Merity et al., 2016) and C4 (Raffel et al., 2020), as well as accuracy for zero-shot tasks. The **Average accuracy** column is the mean of 5 zero-shot task accuracies. Primary metrics are Wiki2 (PPL), C4 (PPL) and Average accuracy.

Size	Method	Avg bits	Wiki2↓	C4↓	WinoGrande↑	PiQA↑	HellaSwag↑	ArcE↑	ArcC↑	Average accuracy↑
7B	–	16.00	5.12	6.63	67.25	78.45	56.69	69.32	40.02	62.35
	AQLM	3.04	5.46	7.10	68.35	76.61	54.36	67.76	38.65	61.15
	GPTQ	3.00	8.28	10.72	60.30	71.65	45.60	56.48	31.23	53.05
	SpQR	2.98	6.21	8.23	63.38	74.27	51.32	62.21	34.13	57.06
	QuIP	3.00	-	-	-	-	-	-	-	-
13B	–	16.00	4.57	6.05	69.61	78.73	59.72	73.27	45.56	65.38
	AQLM	3.026	4.83	6.37	67.64	77.80	58.22	73.48	43.60	64.15
	GPTQ	3.00	5.87	7.90	64.17	75.14	53.70	68.14	39.16	60.06
	SpQR	2.98	5.28	7.07	67.96	76.93	55.72	68.06	38.48	61.43
	QuIP	3.00	5.12	6.79	69.93	76.88	57.07	70.41	41.47	63.15
70B	–	16.00	3.12	4.97	76.95	81.07	63.99	77.74	51.11	70.17
	AQLM	3.01	3.36	5.17	77.19	81.28	63.23	77.61	50.00	69.86
	GPTQ	3.00	4.41	6.26	73.72	78.73	59.79	73.65	44.20	66.02
	SpQR	2.98	3.85	5.63	74.35	80.41	61.65	75.88	46.16	67.69
	QuIP	3.01	3.87	5.67	74.59	79.98	60.73	73.19	46.33	66.96

Table 3: Evaluation of quantized Llama 2 models for **4-4.1 bits per parameter**. The table reports perplexity on Wiki-Text2 (Merity et al., 2016) and C4 (Raffel et al., 2020), as well as accuracy for zero-shot tasks. The **Average accuracy** column is the mean of 5 zero-shot task accuracies. Primary metrics are Wiki2 (PPL), C4 (PPL) and Average accuracy.

Size	Method	Avg bits	Wiki2↓	C4↓	WinoGrande↑	PiQA↑	HellaSwag↑	ArcE↑	ArcC↑	Average accuracy↑
7B	–	16.00	5.12	6.63	67.25	78.45	56.69	69.32	40.02	62.35
	AQLM	4.044	5.21	6.74	67.32	77.69	56.10	68.90	40.27	62.06
	GPTQ	4.000	5.49	7.20	67.17	76.82	55.17	67.42	40.02	61.32
	SpQR	3.980	5.28	6.87	66.54	77.42	55.97	68.14	39.85	61.58
	QuIP	4.000	-	-	-	-	-	-	-	-
13B	QuIP#	4.020	5.29	6.86	66.85	77.91	55.78	68.06	39.68	61.66
	–	16.00	4.57	6.05	69.61	78.73	59.72	73.27	45.56	65.38
	AQLM	3.938	4.64	6.14	70.40	78.56	59.23	72.22	43.94	64.87
	GPTQ	4	4.78	6.34	68.51	77.48	58.57	69.82	42.58	63.39
	SpQR	3.980	4.69	6.20	68.82	78.13	59.11	72.90	44.62	64.72
70B	QuIP	4.00	4.76	6.29	69.69	79.00	58.91	73.27	44.88	65.15
	QuIP#	4.011	4.68	6.20	69.38	77.91	58.86	73.74	44.63	64.90
	–	16.00	3.12	4.97	76.95	81.07	63.99	77.74	51.11	70.17
	AQLM	4.07	3.17	5.01	76.90	81.41	63.64	78.09	51.00	70.21
	GPTQ	4.00	3.34	5.15	75.45	81.56	63.24	76.56	49.57	69.28
	SpQR	3.97	3.24	5.07	76.48	81.12	63.70	76.05	50.34	69.54
	QuIP	4.00	3.58	5.38	76.01	80.25	61.97	74.28	47.01	67.90
	QuIP#	4.01	3.22	5.05	76.80	81.45	63.51	78.37	50.85	70.20

parameter range. One possible explanation for this is that layerwise fine-tuning (defined in Section 3.4) gives the most benefit in regions with lower compression bit width because these regions have higher error in the first place. Conversely, we observe that 3 and 4-bit quantizers are already fairly close to unquantized (FP16) model perplexity.

4.2. Ablation analysis

The AQLM algorithm makes several design choices that need to be validated separately: the initialization, the alternating optimization, the fine-tuning protocol, and the choice of hyperparameters. Here, we study how each of these components affect the overall algorithm.

Initialization. As we discuss in Section 3, we initialize AQLM with residual K-means to obtain a good initial guess for both codes and codebooks. That is, we run K-means for the weight matrix, then subtract the nearest cluster from each weight, and run K-means again M times. A simple baseline would be to initialize all codes uniformly at random. We compare the two initialization strategies for the problem of quantizing a single linear layer within LLAMA 2 70B model to 3 bits per parameter. We quantize groups of 8 consecutive weights using 2 codebooks, 12 bit each. Each codebook contains 2^{12} learnable values. As we can see in Figure 4, AQLM with K-means initialization needs significantly fewer training iterations to achieve the desired loss. The difference is so drastic that we expect that running AQLM with a random initialization would require extremely high runtimes to accurately quantize the largest models.

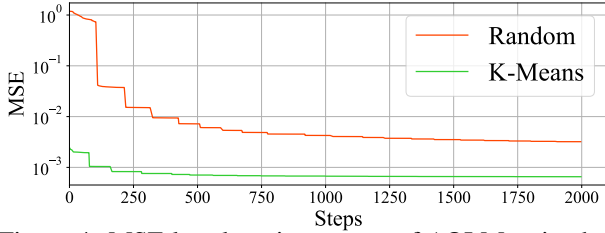


Figure 4: MSE loss learning curves of AQLM trained on the self attention q_proj linear layer of 10-th block in the LLAMA 2 70B model.

Fine-tuning. Next, we validate the fine-tuning procedure. We compare the full block fine-tuning (default) against three alternatives: i) no fine-tuning at all, ii) fine-tuning only non-linear layers (i.e. RMSNorm), but not the AQ parameters, and iii) fine-tuning only the AQ parameters, but not the non-linear layers. Table 4 summarizes our results: fine-tuning the entire model or only AQ parameters achieves competitive performance, while training only RMSNorm scales is comparable to not fine-tuning at all. We attribute these observations to the fact that over 99% of quantized layer parameters are contained in AQ codebooks C_m , whereas the remaining parameters are small 1-dimensional tensors. This validates the use of the AQ approach, as many competing algorithms do not have learnable per-layer codebooks. Notably, QuIP# uses a shared fixed lattice instead. We also note that, even without fine-tuning, AQLM is competitive to previous state-of-the-art results.

Table 4: Ablation analysis of AQLM with different fine-tuning restrictions on Llama-2 7B model at 2.02 bit width.

Name	Wiki2↓	C4↓
w/o	8.18	10.59
RMSnorm	8.31	10.46
AQ params	6.92	8.85
Full	6.93	8.84

Number of samples. Finally, we verify our choice of calibration hyperparameters. Traditionally, most PTQ algorithms use several hundred calibration sequences (e.g. [Frantar et al. \(2022a\)](#) has 128). In our experiments, we evaluate both AQLM and baselines with additional calibration data. Our original motivation for that was to avoid potential overfitting when fine-tuning entire transformer blocks. To test this assumption, we run our algorithm with different calibration set sizes, varying from 128 to 4096 sequences. For each size, we report the average perplexity on WikiText2 over 3 runs, along with standard deviations. The results in Table 5 demonstrate that increasing the number of samples leads to gradual reduction in perplexity with seemingly diminishing returns. Since the perplexity is still monotonically improving from 128 to 4096 samples, it is possible that larger sample sizes would yield further improvements.

Table 5: Wikitext2 PPL as a function of calibration set size for Llama 2 (7B) quantized to 2.3 bits with AQLM, averaged over 3 runs. SD stands for adjusted standard deviation.

# of samples	Average PPL	SD
128	6.994	0.127
256	6.584	0.031
512	6.455	0.005
1024	6.353	0.008
2048	6.297	0.018
4096	6.267	0.005

5. Conclusion and Future Work

We presented AQLM, a variant of additive quantization (AQ) targeted to accurate LLM compression. Specifically, AQLM adapts AQ to the layer-wise quantization problem by making it instance-aware, by taking the layer input distributions into account into the codebook optimization. Moreover, we combine this approach with a block fine-tuning approach, which allows us to further reduce quantization error across layers. To our knowledge, AQLM improves the current state-of-the-art results for LLM quantization in the regime of 2 and 3 bits per weight.

In terms of limitations, AQLM is more computationally-expensive relative to existing direct post-training quantization methods, such as RTN or GPTQ. Moreover, as detailed in the experiments, we have found it to be sensitive to the choice of parameters, such as the number of codebooks, or the initialization of centroids. Further, since it uses a more sophisticated encoding, its implementation will be more complex than direct quantization methods.

In future work, we plan to provide an efficient GPU implementation of AQLM. Further, we intend to conduct a more detailed analysis of the importance of specific parameters on the quality of compression, as well as end-to-end joint fine-tuning of codebook parameters, across the entire model.

6. Acknowledgements

Authors would like to thank Ruslan Svirschevski for his help in solving technical issues with AQLM and baselines. We also thank Tim Dettmers for helpful discussions on the structure of weights in modern LLMs and size-accuracy trade-offs. Finally, authors would like to thank the communities of ML enthusiasts known as LocalLLaMA⁵ and Petals community on discord⁶ for the crowd wisdom about running LLMs on consumer devices.

References

- Babenko, A. and Lempitsky, V. Additive quantization for extreme vector compression. In *Proceedings of the IEEE Conference on Computer Vision and Pattern Recognition*, pp. 931–938, 2014.
- Besag, J. On the statistical analysis of dirty pictures. *Journal of the Royal Statistical Society Series B: Statistical Methodology*, 48(3):259–279, 1986.
- Biderman, S., Schoelkopf, H., Anthony, Q., Bradley, H., O’Brien, K., Hallahan, E., Khan, M. A., Purohit, S., Prashanth, U. S., Raff, E., et al. Pythia: A suite for analyzing large language models across training and scaling. *arXiv preprint arXiv:2304.01373*, 2023.
- Blalock, D. and Gutttag, J. Multiplying matrices without multiplying. In *International Conference on Machine Learning*, pp. 992–1004. PMLR, 2021.
- Burton, D., Shore, J., and Buck, J. A generalization of isolated word recognition using vector quantization. In *ICASSP ’83. IEEE International Conference on Acoustics, Speech, and Signal Processing*, volume 8, pp. 1021–1024, 1983. doi: 10.1109/ICASSP.1983.1171915.
- Chee, J., Cai, Y., Kuleshov, V., and Sa, C. D. Quip: 2-bit quantization of large language models with guarantees, 2023.
- Chen, S., Wang, W., and Pan, S. J. Deep neural network quantization via layer-wise optimization using limited training data. *Proceedings of the AAAI Conference on Artificial Intelligence*, 33(01):3329–3336, Jul. 2019. doi: 10.1609/aaai.v33i01.33013329. URL <https://ojs.aaai.org/index.php/AAAI/article/view/4206>.
- Chen, Y., Guan, T., and Wang, C. Approximate nearest neighbor search by residual vector quantization. *Sensors*, 10(12):11259–11273, 2010.
- Clark, P., Cowhey, I., Etzioni, O., Khot, T., Sabharwal, A., Schoenick, C., and Tafjord, O. Think you have solved question answering? try arc, the ai2 reasoning challenge. *arXiv preprint arXiv:1803.05457*, 2018.
- Computer, T. Redpajama: an open dataset for training large language models, 2023. URL <https://github.com/togethercomputer/RedPajama-Data>.
- Dettmers, T. and Zettlemoyer, L. The case for 4-bit precision: k-bit inference scaling laws. *arXiv preprint arXiv:2212.09720*, 2022.
- Dettmers, T., Lewis, M., Belkada, Y., and Zettlemoyer, L. LLM.int8(): 8-bit matrix multiplication for transformers at scale. *Advances in Neural Information Processing Systems 35: Annual Conference on Neural Information Processing Systems 2022, NeurIPS 2022*, 2022.
- Dettmers, T., Pagnoni, A., Holtzman, A., and Zettlemoyer, L. QLoRA: Efficient finetuning of quantized llms. *arXiv preprint arXiv:2305.14314*, 2023a.
- Dettmers, T., Svirschevski, R., Egiazarian, V., Kuznedelev, D., Frantar, E., Ashkboos, S., Borzunov, A., Hoefler, T., and Alistarh, D. Spqr: A sparse-quantized representation for near-lossless llm weight compression. *arXiv preprint arXiv:2306.03078*, 2023b.
- Fernández-Marqués, J., AbouElhamayed, A. F., Lane, N. D., and Abdelfattah, M. S. Are we there yet? product quantization and its hardware acceleration. *ArXiv*, abs/2305.18334, 2023. URL <https://api.semanticscholar.org/CorpusID:258967539>.
- Frantar, E., Ashkboos, S., Hoefler, T., and Alistarh, D. Gptq: Accurate post-training quantization for generative pre-trained transformers. *arXiv preprint arXiv:2210.17323*, 2022a.
- Frantar, E., Singh, S. P., and Alistarh, D. Optimal Brain Compression: A framework for accurate post-training quantization and pruning. *arXiv preprint arXiv:2208.11580*, 2022b. Accepted to NeurIPS 2022, to appear.
- Gao, L., Tow, J., Biderman, S., Black, S., DiPofi, A., Foster, C., Golding, L., Hsu, J., McDonnell, K., Muenighoff, N., Phang, J., Reynolds, L., Tang, E., Thite, A., Wang, B., Wang, K., and Zou, A. A framework for few-shot language model evaluation, September 2021. URL <https://doi.org/10.5281/zenodo.5371628>.
- Ge, T., He, K., Ke, Q., and Sun, J. Optimized product quantization. *IEEE transactions on pattern analysis and machine intelligence*, 36(4):744–755, 2013.

⁵<https://www.reddit.com/r/LocalLLaMA/>

⁶<https://github.com/bigscience-workshop/petals/>

- Gholami, A., Kim, S., Dong, Z., Yao, Z., Mahoney, M. W., and Keutzer, K. A survey of quantization methods for efficient neural network inference. *arXiv preprint arXiv:2103.13630*, 2021.
- Gray, R. Vector quantization. *IEEE ASSP Magazine*, 1(2): 4–29, 1984. doi: 10.1109/MASSP.1984.1162229.
- Hubara, I., Nahshan, Y., Hanani, Y., Banner, R., and Soudry, D. Accurate post training quantization with small calibration sets. In *International Conference on Machine Learning (ICML)*, 2021.
- Jegou, H., Douze, M., and Schmid, C. Product quantization for nearest neighbor search. *IEEE transactions on pattern analysis and machine intelligence*, 33(1):117–128, 2010.
- Kim, S., Hooper, C., Gholami, A., Dong, Z., Li, X., Shen, S., Mahoney, M. W., and Keutzer, K. Squeezellm: Dense-and-sparse quantization. *arXiv preprint arXiv:2306.07629*, 2023.
- Kingma, D. P. and Ba, J. Adam: A method for stochastic optimization. *International Conference on Learning Representations (ICLR)*, 2015.
- Li, Y., Gong, R., Tan, X., Yang, Y., Hu, P., Zhang, Q., Yu, F., Wang, W., and Gu, S. BRECCQ: Pushing the limit of post-training quantization by block reconstruction. In *International Conference on Learning Representations (ICLR)*, 2021.
- Li, Z., Ni, B., Zhang, W., Yang, X., and Gao, W. Performance guaranteed network acceleration via high-order residual quantization, 2017.
- Lin, J., Tang, J., Tang, H., Yang, S., Dang, X., and Han, S. Awq: Activation-aware weight quantization for llm compression and acceleration. *arXiv preprint arXiv:2306.00978*, 2023.
- Martinez, J., Clement, J., Hoos, H. H., and Little, J. J. Revisiting additive quantization. In *Computer Vision—ECCV 2016: 14th European Conference, Amsterdam, The Netherlands, October 11–14, 2016, Proceedings, Part II 14*, pp. 137–153. Springer, 2016.
- Martinez, J., Zakhmi, S., Hoos, H. H., and Little, J. J. Lsq++: Lower running time and higher recall in multi-codebook quantization. In *Proceedings of the European Conference on Computer Vision (ECCV)*, pp. 491–506, 2018.
- McCarter, C. and Dronen, N. Look-ups are not (yet) all you need for deep learning inference. *ArXiv*, abs/2207.05808, 2022. URL <https://api.semanticscholar.org/CorpusID:250491319>.
- Merity, S., Xiong, C., Bradbury, J., and Socher, R. Pointer sentinel mixture models. *arXiv preprint arXiv:1609.07843*, 2016.
- Nagel, M., Amjad, R. A., Van Baalen, M., Louizos, C., and Blankevoort, T. Up or down? Adaptive rounding for post-training quantization. In *International Conference on Machine Learning (ICML)*, 2020.
- Norouzi, M. and Fleet, D. J. Cartesian k-means. In *Proceedings of the IEEE Conference on computer Vision and Pattern Recognition*, pp. 3017–3024, 2013.
- Ozan, E. C., Kiranyaz, S., and Gabbouj, M. Competitive quantization for approximate nearest neighbor search. *IEEE Transactions on Knowledge and Data Engineering*, 28(11):2884–2894, 2016. doi: 10.1109/TKDE.2016.2597834.
- Park, G., Park, B., Kwon, S. J., Kim, B., Lee, Y., and Lee, D. nuQmm: Quantized matmul for efficient inference of large-scale generative language models. *arXiv preprint arXiv:2206.09557*, 2022.
- Paszke, A., Gross, S., Massa, F., Lerer, A., Bradbury, J., Chanan, G., Killeen, T., Lin, Z., Gimelshein, N., Antiga, L., Desmaison, A., Kopf, A., Yang, E., DeVito, Z., Raison, M., Tejani, A., Chilamkurthy, S., Steiner, B., Fang, L., Bai, J., and Chintala, S. PyTorch: An imperative style, high-performance deep learning library. In *Conference on Neural Information Processing Systems (NeurIPS)*. 2019.
- Raffel, C., Shazeer, N., Roberts, A., Lee, K., Narang, S., Matena, M., Zhou, Y., Li, W., and Liu, P. Exploring the limits of transfer learning with a unified text-to-text transformer. *Journal of Machine Learning Research*, 21 (140):1–67, 2020.
- Sakaguchi, K., Bras, R. L., Bhagavatula, C., and Choi, Y. Winogrande: an adversarial winograd schema challenge at scale. *Commun. ACM*, 64(9):99–106, 2021. doi: 10.1145/3474381. URL <https://doi.org/10.1145/3474381>.
- Scao, T. L., Fan, A., Akiki, C., Pavlick, E., Ilić, S., Hesslow, D., Castagné, R., Luccioni, A. S., Yvon, F., Gallé, M., et al. Bloom: A 176b-parameter open-access multilingual language model. *arXiv preprint arXiv:2211.05100*, 2022.
- Tata, S. and Patel, J. M. PiQA: An algebra for querying protein data sets. In *International Conference on Scientific and Statistical Database Management*, 2003.
- TII UAE. The Falcon family of large language models. <https://huggingface.co/tiiuae/falcon-40b>, May 2023.

- Touvron, H., Lavril, T., Izacard, G., Martinet, X., Lachaux, M.-A., Lacroix, T., Rozière, B., Goyal, N., Hambro, E., Azhar, F., et al. Llama: Open and efficient foundation language models. *arXiv preprint arXiv:2302.13971*, 2023.
- Tseng, A., Chee, J., Sun, Q., Kuleshov, V., and Sa, C. D. Quip#: Quip with lattice codebooks.
- Vaswani, A., Shazeer, N., Parmar, N., Uszkoreit, J., Jones, L., Gomez, A. N., Kaiser, L., and Polosukhin, I. Attention is all you need. *arXiv preprint arXiv:1706.03762*, 2017.
- Wang, P., Chen, Q., He, X., and Cheng, J. Towards accurate post-training network quantization via bit-split and stitching. In *International Conference on Machine Learning (ICML)*, 2020.
- Xiao, G., Lin, J., Seznec, M., Demouth, J., and Han, S. Smoothquant: Accurate and efficient post-training quantization for large language models. *arXiv preprint arXiv:2211.10438*, 2022.
- Yao, Z., Aminabadi, R. Y., Zhang, M., Wu, X., Li, C., and He, Y. Zeroquant: Efficient and affordable post-training quantization for large-scale transformers. *arXiv preprint arXiv:2206.01861*, 2022.
- Zellers, R., Holtzman, A., Bisk, Y., Farhadi, A., and Choi, Y. Hellaswag: Can a machine really finish your sentence? In Korhonen, A., Traum, D. R., and Màrquez, L. (eds.), *Proceedings of the 57th Conference of the Association for Computational Linguistics, ACL 2019, Florence, Italy, July 28- August 2, 2019, Volume 1: Long Papers*, pp. 4791–4800. Association for Computational Linguistics, 2019. doi: 10.18653/v1/p19-1472. URL <https://doi.org/10.18653/v1/p19-1472>.
- Zhang, S., Roller, S., Goyal, N., Artetxe, M., Chen, M., Chen, S., Dewan, C., Diab, M., Li, X., Lin, X. V., et al. Opt: Open pre-trained transformer language models. *arXiv preprint arXiv:2205.01068*, 2022.
- Zhang, T., Du, C., and Wang, J. Composite quantization for approximate nearest neighbor search. In *International Conference on Machine Learning*, pp. 838–846. PMLR, 2014.
- Zhou, S.-C., Wang, Y.-Z., Wen, H., He, Q.-Y., and Zou, Y.-H. Balanced quantization: An effective and efficient approach to quantized neural networks. *Journal of Computer Science and Technology*, 32(4):667–682, Jul 2017. ISSN 1860-4749. doi: 10.1007/s11390-017-1750-y. URL <https://doi.org/10.1007/s11390-017-1750-y>.